Acta Oceanol. Sin., 2018, Vol. 37, No. 1, P. 89–96
DOI: 10.1007/s13131-018-1160-1
http://www.hyxb.org.cn
E-mail: hyxbe@263.net

The distribution and composition of hydrocarbons in sediments of the South Mid-Atlantic Ridge

HUANG Xin[1]*, CHEN Shuai[2, 3], WANG Xiaoyuan[2, 3], ZHANG Shuwen[1], CHEN Fajin[1], PU Xiaoqiang[1]

[1] Guangdong Province Key Laboratory of Coastal Ocean Variation and Disaster Prediction, Guangdong Ocean University, Zhanjiang 524088, China

[2] Key Laboratory of Marine Geology and Environment, Institute of Oceanology, Chinese Academy of Sciences, Qingdao 266071, China

[3] Laboratory for Marine Mineral Resources, Qingdao National Laboratory for Marine Science and Technology, Qingdao 266071, China

Received 11 May 2017; accepted 31 May 2017

Abstract

Sediment samples obtained from the South Mid-Atlantic Ridge are analyzed by a gas chromatography-mass spectrometer (GC-MS) for the abundances and distributions of hydrocarbons. The hydrocarbons in the samples exhibit a bimodal distribution of *n*-alkanes and are rich in 3-methylalkanes, 8-methylalkanes and 2, 4, (*n*-1)-trimethylalkanes, which may be the result of metabolic activity of benthic microorganism. Terpanes, hopanes and steranes are all enriched in the samples, which also support the microbial origin of hydrocarbons in samples. Bitumen and hydrocarbons in the samples show a trend that the contents are the highest in the Samples 22V-TVG10 and 26V-TVG05 collected near hydrothermal areas, and the lowest in samples 22IV-TVG01, 22V-TVG11, and 22V-TVG14 collected far from the hydrothermal areas, which suggest the possible influence on the samples by hydrothermal activity.

Key words: hydrocarbons, South Mid-Atlantic Ridge, sediment, hydrothermal activity

Citation: Huang Xin, Chen Shuai, Wang Xiaoyuan, Zhang Shuwen, Chen Fajin, Pu Xiaoqiang. 2018. The distribution and composition of hydrocarbons in sediments of the South Mid-Atlantic Ridge. Acta Oceanologica Sinica, 37(1): 89–96, doi: 10.1007/s13131-018-1160-1

1 Introduction

The study of hydrocarbons in the geologic environment has been paid wide attention by many researchers (Simoneit et al., 1979, 1990, 2004; Chernova et al., 2001; Lein et al., 2003; Venkatesan et al., 2003; Petrova et al., 2010; Peng et al., 2011; Morgunova et al., 2012). The discovery of hydrothermal activity provided a novel impetus to the further study of hydrocarbons in the geologic environment (Zhang et al., 2001; Lein et al., 2003; Simoneit et al., 2004; Peng et al., 2011). In recent years, many researchers tried to judge the origin of hydrocarbons and assess the influence on hydrothermal products by hydrothermal activity. For example, Lein et al. (2003) and Simoneit et al. (2004) analyzed the distribution and composition of hydrocarbons and other organic matter in hydrothermal sulfide and sediment in Rainbow hydrothermal fields, and suggested the microorganisms related to hydrothermal activity might be the origin of organic matter in hydrothermal sulfide and sediment; Morgunova et al. (2012) discovered that the contents of hydrocarbons in hydrothermal sediments was much higher than those in pelagic sediments around Ashadze hydrothermal field, and considered the thermal degradation of macromolecule organic matters in hydrothermal system might be the reason of the enrichment of hydrocarbons in hydrothermal sediments.

The slow-spreading Mid-Atlantic Ridge, which accounts for about 40% of the total length of global mid-ocean ridges, stretches from 87°N (≈330 km from the North Pole) to 54°S. The Mid-Atlantic Ridge is divided into the North Mid-Atlantic Ridge and the South Mid-Atlantic Ridge by the Romanche Trench near the equator. The South Mid-Atlantic Ridge turns towards the Atlantic -Indian Ridge near 54°S, crosses the Crozet Plateau, and continues eastwards to the Southwest Indian Ridge.

In recent years, scientists have discovered several hydro-

Foundation item: The National Basic Research Program (973 Program) of China under contract No. 2013CB429700; the National Natural Science Foundation of China under contract Nos 41476044, 41325021, 41676008 and 41476010; the Special Fund for the Taishan Scholar Program of Shandong Province under contract No. ts201511061; the AoShan Talents Program supported by Qingdao National Laboratory for Marine Science and Technology under contract No. 2015ASTP-0S17; the Program for Key Basic Research of the Ministry of Science and Technology under contract No. 2016YFC1401403; the Foundation for Distinguished Young Teacher in Higher Education of Guangdong under contract No. Yq2014004; the Guangdong Natural Science Foundation of China under contract No. 2016A030312004; the International Science and technology cooperation project of China under contract No. GASI-IPOVAI-04; the Open Fund of the Key Laboratory of Marine Geology and Environment, Chinese Academy of Sciences under contract No. MGE2015KG04; the Open Fund of the Key Laboratory of Submarine Geosciences, State Oceanic Administration of China under contract No. KSLG1503; the Program for Scientific Research Start-up Funds of Guangdong Ocean University under contract No. E15169.

*Corresponding author, E-mail: shaoshanhx@126.com

thermal areas in the South Mid-Atlantic Ridge. In 2009, two new hydrothermal areas between the 13°–14°S segments of the South Mid-Atlantic Ridge were found during the DY115-21 cruise, and hydrothermal sulfide chimney samples were obtained (Tao et al., 2011). In 2010–2012, the DY115-22 and DY115-26 cruises continued to investigate the South Mid-Atlantic Ridge, and a variety of hydrothermal sulfides, sediment, and rocks were collected. During these cruises, the sampling locations (except 22V-TVG14) are centered along the South Mid-Atlantic Ridge between 12° and 15°S (Fig. 1), where the spreading rate is about 3.4 cm/a (DeMets et al., 1994).

In this study, we measured the abundance and distribution of hydrocarbons of ten sediment samples collected along the South Mid-Atlantic Ridge, and compared the hydrocarbons in sediments collected at different distances from the hydrothermal field. Our goal is to identify the main source of hydrocarbons in the samples, and assess the influence on hydrocarbons by hydrothermal activities in the sediments.

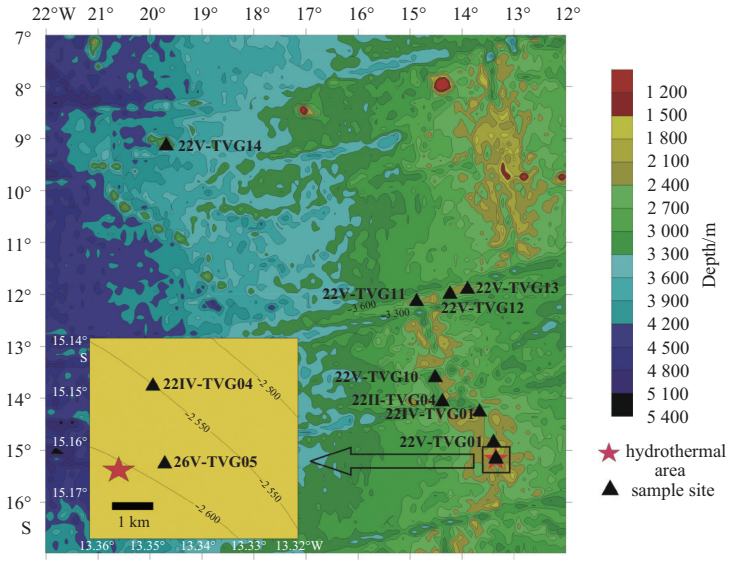

Fig. 1. Sample collection sites along the South Mid-Atlantic Ridge.

2 Sampling and analyses

In 2010–2012, samples were collected using a TV-grab during the DY115-22 and DY115-26 cruises aboard the R/V *Dayang Yihao* conducted by the China Ocean Mineral Resources Research and Development Association along the South Mid-Atlantic Ridge. The sites, water depths and descriptions of samples are summarized in Table 1 and Fig. 1.

Calcite was the dominating mineral component in all samples (Fig. 2), and a small amount of kaolinite, which might be terrgenous input (Simoneit, 1977), was detected in 22II-TVG04 and 22V-TVG10.

After collection, the samples were placed in bags and stored at –20°C until analysis. Sediment (200 g) from each sample was placed into dry acid-cleaned glass beakers, and dried at 40°C for 48 h. The dried sediment was powdered in an agate mortar to 100 meshes and dried for at 40°C for a further 24 h.

The extraction and analysis of hydrocarbons were performed at the Lanzhou Center for Oil and Gas Resources, Institute of Geology and Geophysics, Chinese Academy of Sciences. The extraction process was as follows: bitumen was extracted using a Soxhlet extractor with chloroform for 72 h. *n*-hexane was used to remove asphaltene and solubilize organic matter. Soluble organic matter was separated by a column chromatography (silica-gel 60; inner diameter 5 mm; length 35 mm), and then analyzed by a gas chromatography-mass spectrometry (GC-MS).

A 6890N gas chromatography analyzer (HP 6890 GC plus trace-MS selective detector) with a 30-m DB-5MS fused silica capillary column (inner diameter 0.2 mm; film thickness 0.2 μm) was used. The carrier gas was helium. The GC temperature program used was as follows: injection at 80°C, 2 min isothermal; from 80 to 290°C at 4°C/ min; 20 min isothermal. The MS (5973N) was operated in EI model at 70 eV.

Table 1. Sample locations and principal characteristics

Sample No.	West longitude(°)	South latitude(°)	Depth/m	Distance from hydrothermal vent/km	Brief characteristics
22II-TVG04	14.4	14.1	2 634	163.1	yellowish-brown, high viscosity, small grain
22IV-TVG01	13.7	14.3	2 246	105.3	pale yellow, low viscosity
22IV-TVG04	13.3	15.1	2 888	2.2	dark brown with a little white shell
22V-TVG01	13.4	14.8	2 481	44.5	yellowish-brown with black solid particles
22V-TVG10	14.5	13.6	2 949	21.4	dark brown, high viscosity
22V-TVG11	14.9	12.1	2 641	381.3	dark grey, cohesionless
22V-TVG12	14.2	12.0	2 814	366.7	dark mahogany, high viscosity
22V-TVG13	13.9	11.9	2 316	371.3	mahogany, medium viscosity
22V-TVG14	19.7	9.1	1 527	964.7	off-white, cohesionless, large grain
26V-TVG05	13.3	15.2	2 854	0.9	dark brown, high viscosity, small grain

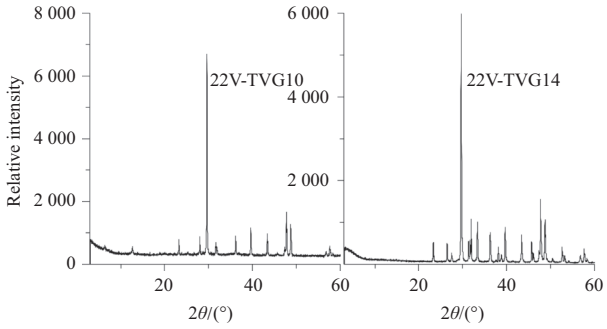

Fig. 2. XRD spectra of the representative samples.

3 Results

3.1 *Bitumen*

The concentration of bitumen in the samples ranged from 20.23×10^{-6} to 87.74×10^{-6} (Table 2), and the concentration was the highest in Sample 22V-TVG10, followed by Sample 26V-TVG05. The concentrations of bitumen in Samples 22V-TVG10 and 26V-TVG05 were corresponded to the values in carbonate sediments (59.88×10^{-6}) of Logatchev hydrothermal field on the North Mid-Atlantic Ridge (Peng et al., 2011).

3.2 *n-alkanes*

The concentrations of *n*-alkanes were between 2.22×10^{-3} and 1.88×10^{-6} (Table 3). They were the highest in Samples 22V-TVG10 and 26V-TVG05, and the lowest in Sample 22V-TVG13. *n*-alkane lengths ranged from carbon number 15 to 33 (n-pentadecane was not detected in Sample 22V-TVG14). The *n*-alkanes in the samples exhibited a bimodal pattern (Fig. 3), and the CPI (carbon preference index) in the samples ranged from 1.04 to 1.52. The ratios between short-chain ($\leqslant C_{21}$) and long-chain ($>C_{21}$) *n*-alkanes ranged from 0.26 to 1.42. The short-chain *n*-alkanes possessed obvious advantage of even carbon number with C_{16} or C_{18} as the maximum (C_{17} in Sample 22V-TVG13), and the values of OEP17 (odd-even-predominance at C_{17}, Table 3) were between 0.66 and 1.05. However, the long-chain *n*-alkanes possessed the obvious advantage of an odd carbon number with C_{29} or C_{31} as the maximum, and the values of OEP29 (odd-even-predominance at C_{29}, Table 3) were between 1.80 and 3.56.

3.3 *Branched alkanes*

The concentrations of three kinds of branched alkanes (3-methylalkane, 8-methylalkanes and 2, 4, (*n*-1)-trimethylalkanes) in all samples were high, and the concentration of the latter was the highest in all samples except 22V-TVG11.

The 3-methylalkanes ranged from C_{16}–C_{24}, and exhibited an unimodal pattern with maximum carbon number at 19 (Table 3). The structures of mass spectra of 3-methylalkanes were similar with the same carbon number *n*-alkanes. The mass spectra exhibited a base peak at *m/z*=57 (mass-to-charge ratio), and intense key ion at *m/z* =211, 225, 239, 267, 281, 295, 309 and so on, with typical ethyl [(M^+(Mass)=29)] cleavage (Fig. 4a).

The 8-methylalkanes ranged from C_{17} to C_{31}, with maximum carbon number at 19 and only odd carbon numbered homologs (Table 3). The mass spectra of 8-methylalkanes exhibited a base peak at *m/z*=127, and intense key ion at *m/z*=239, 267, 295, 323, 351, 379, 407 and so on (Fig. 4b).

The 2, 4, (*n*-1)-trimethylalkanes ranged from C_{14} to C_{30}, with maximum carbon number at 18 and only even carbon numbered homologs (Table 3). The mass spectra exhibited a base peak at *m/z*=85, and intense key ion at *m/z*=197, 225, 253, 281, 309, 337 and so on, with typical isopropyl (M^+=29) cleavage (Fig. 4c).

The concentrations of phytane and pristane were between 0.037×10^{-6} and 0.74×10^{-6}, and their ratios ranged from 0.69 to 1.01. Squalene was detected in high concentration in all samples. The concentrations in samples 22V-TVG10 and 26V-TVG05 were 0.43×10^{-6} and 0.79×10^{-6} respectively, which demonstrates that the samples were affected by microorganism. Nor-pristane was present in some samples, but the content was lower than those of phytane and pristane.

3.4 *Cyclic biomarkers*

The cyclic biomarkers present in all samples were tricyclic terpanes, hopanes and steranes, and most samples had similar triterpane compositions. The peaks in the chromatogramat *m/z* 191 (Fig. 5) indicate the presence of tricyclic, tetracyclic and pentacyclic triterpanes. The dominant terpanes were hopanes (17α(H), 21β(H)-hopane series) and moretanes (17β(H), 21α(H)-hopane series). The 17α(H), 21β(H)-hopane series ranges from C_{27} to C_{35} (C_{28} absent) with a maxima of C_{29} and C_{30}.

C_{27}, C_{28} and C_{29} steranes were also detected, and the content followed the same distribution law in all samples: $C_{29}>C_{27}>C_{28}$ (Fig. 6). The ratios between C_{27} and C_{29} steranes were 0.50–0.87. C_{30} 4-methylsteranes detected in the samples probably derive from methanotrophs (Suzuki et al., 1987); Peng et al. (2011) reported that C_{30} 4-methylsteranes lived around hydrothermal vents, and might be an indicator of hydrothermal activity. Diasteranes (C_{27} to C_{29}) and pregnane were present in low amounts; they usually are present in highly mature condensates (Suzuki et al., 1987).

4 Discussion

4.1 *The origin of hydrocarbons*

The compositions of hydrocarbons in the samples were simil-

Table 2. Compositions of organic matter in the sediment samples

Sample No.	Mass of sample/g	Mass of bitumen/g	Concentration of bitumen/10^{-6}	Mass of alkanes/g	Concentration of alkanes/10^{-6}
22II-TVG04	105	0.004 23	40.28	0.000 88	8.38
22IV-TVG01	116	0.003 61	31.12	0.000 33	2.84
22IV-TVG04	91	0.002 75	30.22	0.000 85	9.34
22V-TVG01	105	0.003 47	33.05	0.001 09	10.38
22V-TVG10	115	0.010 09	87.74	0.004 41	38.35
22V-TVG11	95	0.002 66	28.00	0.000 27	2.84
22V-TVG12	130	0.002 63	20.23	0.000 78	6.00
22V-TVG13	127	0.006 93	54.57	0.001 50	11.81
22V-TVG14	112	0.002 79	24.91	0.000 58	5.18
26V-TVG05	96	0.005 99	62.40	0.002 81	29.27

Table 3. Composition of alkanes in the sediment samples

Alkanes/ng·g^{-1}	Sample									
	22II-TVG04	22IV-TVG01	22IV-TVG04	22V-TVG01	22V-TVG10	22V-TVG11	22V-TVG12	22V-TVG13	22V-TVG14	26V-TVG05
Pentadecane	8	2	12	36	437	2	8	26	nd	120
2, 4, 15-Trimethyl-tetradecane	12	nd	nd	nd	444	nd	nd	nd	nd	207
3-Methyl-pentadecane	8	nd	nd	nd	315	nd	nd	nd	nd	220
Hexadecane	156	10	144	266	1 880	10	68	360	28	828
Nor-pristane	51	nd	49	79	nd	nd	18	132	7	204
3-Methyl-hexadecane	44	nd	61	97	303	nd	24	96	5	286
Heptadecene	183	17	237	194	941	9	74	94	39	713
Heptadecane	195	44	261	282	913	36	160	584	138	660
Pristane	193	47	250	372	525	37	121	449	130	616
2, 4, 15-Trimethyl-hexadecane	552	97	690	547	1 878	58	290	678	216	1 828
3-Methyl-heptadecane	277	61	287	231	652	32	144	338	99	754
Octadecane	320	99	344	352	1 131	83	229	532	340	865
8-Methyl-heptadecane	303	80	467	305	982	42	186	437	168	1 227
Phytase	228	66	247	469	591	51	213	577	188	745
3-Methyl-octadecane	144	38	223	113	438	25	102	195	81	455
Nonadecene	305	90	374	296	1 171	38	184	246	170	1 010
Nonadecane	117	54	164	123	563	45	139	224	166	359
2, 4, 17-Trimethyl-octadecane	588	167	782	495	2 395	120	430	730	331	2 009
3-Methyl-nonadecane	211	74	280	183	889	49	151	234	117	714
Eicosane	112	52	156	118	539	48	119	201	133	388
8-Methyl-nonadecane	369	115	543	366	1 294	86	278	509	213	1 329
3-Methyl-eicosane	166	41	183	135	226	21	44	111	81	443
Heneicosene	137	46	218	159	578	23	122	151	78	525
Heneicosane	49	39	107	79	550	34	75	120	106	207
2, 4, 19-Trimethyl-eicosane	385	130	554	487	1 908	109	371	536	212	1 529
3-Methyl-uneicosane	128	43	207	147	568	32	123	192	69	579
Docosane	77	45	118	107	295	45	84	121	135	288
8-Methyl-uneicosane	273	90	366	326	1 200	79	254	375	139	1 043
3-Methyl-doeicosane	106	37	105	103	578	28	86	166	63	380

to be continued

Continued from Table 3

Alkanes/ng·g^{-1}	Sample									
	22II-TVG04	22IV-TVG01	22IV-TVG04	22V-TVG01	22V-TVG10	22V-TVG11	22V-TVG12	22V-TVG13	22V-TVG14	26V-TVG05
Tricosane	67	38	83	69	380	50	84	119	125	341
2, 4, 21-Trimethyl-docosane	182	63	236	303	1 170	59	189	253	101	789
3-Methyl-tricosane	39	13	73	71	382	18	41	68	30	204
Tetracosane	45	43	69	100	242	64	66	114	132	259
8-Methyl-tricosane	133	49	167	230	922	57	140	241	83	684
Pentacosane	117	75	121	296	501	101	132	236	175	697
2, 4, 23-Trimethyl-tetracosane	98	41	87	154	852	37	90	142	38	390
Hexacosane	78	51	56	159	282	89	70	139	100	249
8-Methyl-pentacosane	104	33	85	128	728	37	92	133	48	409
Squalene	156	236	101	318	426	269	129	179	282	787
Heptacosane	164	80	95	238	490	120	111	245	124	426
2, 4, 25-Trimethyl-hexacosane	68	22	42	95	631	23	44	108	nd	326
Octacosane	83	49	48	129	252	96	44	163	73	176
8-Methyl-heptacosane	79	24	61	137	719	30	60	112	nd	308
Nonacosane	300	139	165	428	1 099	218	184	295	143	685
2, 4, 27-Trimethyl-octacosane	54	18	45	172	654	nd	42	108	nd	231
Triacontane	104	49	49	125	355	98	53	104	78	186
8-Methyl-nonacosane	103	19	48	92	677	nd	45	95	nd	228
Hentriacontane	424	130	139	408	1 392	255	174	301	107	599
2, 4, 29-Trimethyl-triacontane	nd	10	nd	nd	297	nd	nd	nd	nd	nd
8-Methyl- hentriacontane	nd	12	nd	nd	410	nd	nd	nd	nd	nd
Dotriacontane	92	14	43	81	350	41	20	64	24	207
Tritriacontane	161	29	54	144	649	26	63	109	21	346
$C_{21-}/_{C22+}$	0.63	0.50	1.42	0.63	1.05	0.26	0.88	1.15	0.95	0.89
CPI[1)]	1.42	1.49	1.14	1.40	1.21	1.52	1.45	1.22	1.05	1.22
OEP17[2)]	0.68	0.74	0.90	0.75	0.54	0.70	0.93	1.05	0.68	0.66
OEP29[3)]	3.18	2.65	3.19	3.17	3.49	2.18	3.56	2.16	1.80	3.55
Pr/Ph[4)]	0.85	0.72	1.01	0.79	0.89	0.72	0.57	0.78	0.69	0.83

Note: nd indicates not detected, C_{21-} short-chain ($\leqslant C_{21}$), C_{22+} long-chain ($>C_{21}$), CPI[1)] carbon preference index for *n*-alkanes is odd/even *n*-alkanes in the carbon range from C_{15} to C_{33}, OEP17[2)] $[m(C_{15})+6m(C_{17})+m(C_{19})]/[4m(C_{16})+4m(C_{18})]$, OEP29[3)] $[m(C_{27})+6m(C_{29})+m(C_{31})]/[4m(C_{28})+4m(C_{30})]$; [4)] pristine; and Ph phytane.

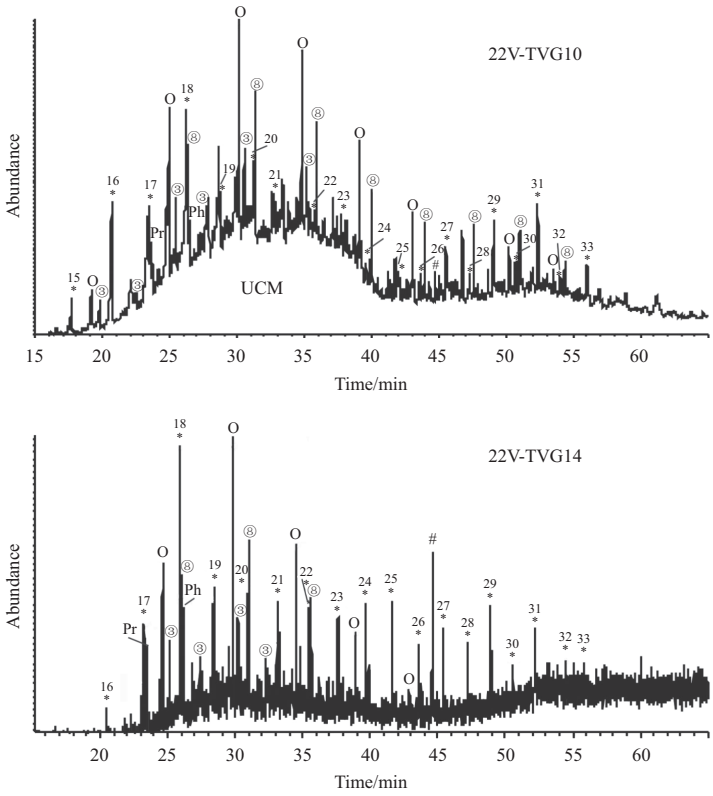

Fig. 3. Gas chromatograms of alkanes of representative samples. Numbers refer to the carbon chain length of *n*-alkanes; O represents trimethyl-alkane, ③ 3-methylalkanes, ⑧ 8-methylalkanes, # Squalene, Pr pristane, Ph phytane, and UCM unresolved complex mixture.

ar between each other, suggesting the similar source of hydrocarbons in the samples. The distributions and compositions of the *n*-alkanes in the samples exhibit an odd to even predominance of high molecular mass compounds and show a bimodal distribution (Fig. 7), which are the characteristic of terrigenous input, and indicate a terrigenous source of the high molecular mass *n*-alkanes (Elias et al., 1997). Simoneit (1977) confirmed that seafloor sediments were affected by eolian dusts at 35°N and 30°S in the South Atlantic. Therefore, the terrigenous input in this study might be also derived from eolian dusts.

The low molecular mass *n*-alkanes show an even to odd predominance with maxima at C_{16} and C_{18} (Fig. 7); this result suggests that the benthic microorganisms may be the main source of low molecular mass *n*-alkanes in the samples (Simoneit et al., 2004).

The isoprenoid alkenes in the samples may have originated from cell membranes of bacteria or archaea (Kates, 1997). The steranes in the samples may be the result of submarine macromolecular (e.g., cholesterol) thermal alteration; hopanes likely originate from microbial macromolecules (Simoneit et al., 2004). The presence of these typical biomarkers supports the biological origin of organic matter in the samples.

4.2 *The influence of hydrothermal activity*

Hydrothermal systems are characterized by sufficiently high nutritious and energetic potentials to form and maintain the occurrence of numerous biological communities constituting the so-called "oasis of life" (Yamanaka and Sakata, 2004; Li et al., 2011; Morgunova et al., 2012). The biomass and organic content in sediment near hydrothermal vents are usually several orders of magnitude higher (Yamanaka and Sakata, 2004; Morgunova et al., 2012). The concentration of bitumen can be used as biomass and productivity indicators (Morris and Culkin, 1976; Simoneit et al., 2004). The contents of bitumen in Samples 22V-TVG10 and 26V-TVG05 (similar to the values (59.88×10^{-6}) in carbonate sediments of Logatchev hydrothermal field), were much higher than those in sample 22V-TVG14 which was collected far from hydrothermal field (Table 2). Huang et al. (2017) analyzed the sediment core samples from the northern Okinawa Trough, and discovered that the contents of bitumen in samples affected by hydrothermal activity were higher than the value in samples without the influence of hydrothermal activity. Therefore, the samples which were collected near hydrothermal field (e.g., Samples 22V-TVG10 and 26V-TVG05) might be under the influence of hydrothermal activity.

Peng et al. (2011) pointed out that *n*-hexadecane and *n*-octadecane in sediment around hydrothermal field might be related to sulfur metabolism; the *n*-alkanes (especially *n*-hexadecane and *n*-octadecane) in Samples 22V-TVG10 and 26V-TVG05 were higher than those in other samples, suggesting that part of n-alkanes might be derived from sulfur metabolism microorganisms, and also indicating that the samples, especially the samples near the hydrothermal field, may be affected by hydrothermal activity.

However, several samples (e.g., 22IV-TVG04) near the hydrothermal fields had no the characteristics as Samples 22V-TVG10 and 26V-TVG05, which might be related to a sedimentation rate, a hydrothermal plume altitude and a current direction (Brault et al., 1984).

Therefore, hydrocarbons in the samples may mainly origin from metabolic activity of benthic microorganism; meanwhile,

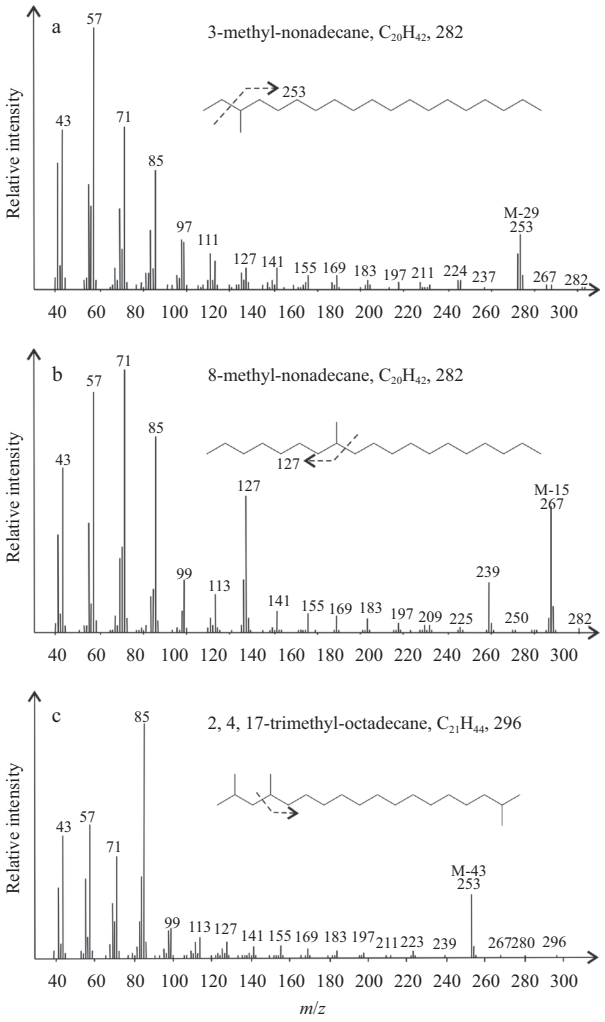

Fig. 4. Representative mass spectra of branched alkanes. a. 3-methylalkane, b. 8-methylalkane, and c. 2, 4, (n-1)-trimethylalkane.

the compositions of hydrocarbons in samples make us difficult to ignore the possible influence by hydrothermal activity.

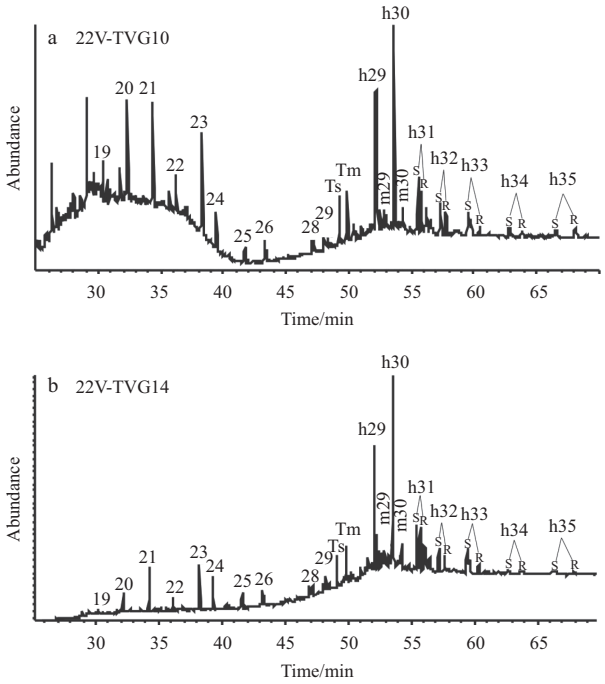

Fig. 5. Mass fragmentogram (m/z 191) in representative samples. Numbers refer to the carbon number of terpanes; h represents hopane and m moretane.

5 Conclusions

Comparison of the distribution characteristics of hydrocarbons in sediment near hydrothermal fields and in sediment far from hydrothermal fields reveals the influence of hydrothermal activity on sediment around hydrothermal fields. The distributions and compositions of n-alkanes in the samples indicate that the hydrocarbons in the samples may mainly origin from metabolic activity of benthic microorganism. The contents of bitumen in samples collected near hydrothermal field were much higher than those in sample collected far from the hydrothermal field, which shows that the biomass is higher in sediment near hydrothermal field, and suggests that the samples, especially the samples collected near the hydrothermal field, mat be affected by hydrothermal activity. The distribution and composition of hy-

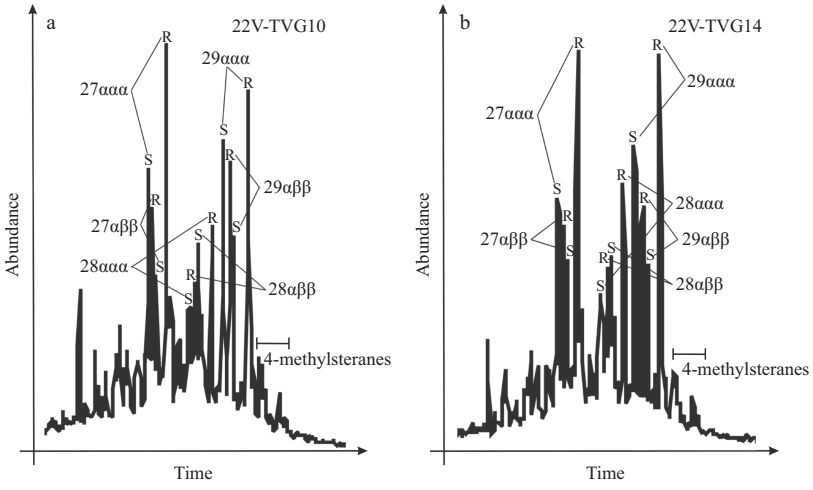

Fig. 6. Mass fragmentogram (m/z 217) in representative samples.

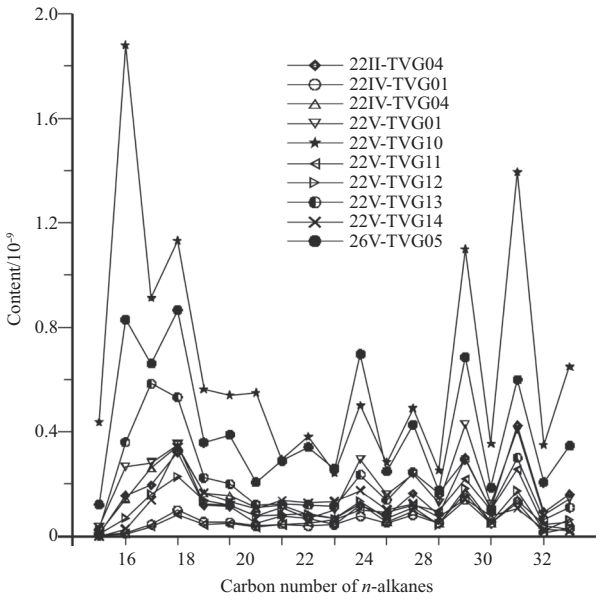

Fig. 7. *n*-alkane distribution in samples (dry sediment).

drocarbons in the samples may be the result of a combination of submarine microorganisms and submarine macromolecular thermal alteration.

Acknowledgements

The authors thank the crews of the COMRA cruise (DY115-22 and DY115-26) for their help with sampling operations, as well as Meng Qianxiang for his help with sampling analysis.

References

Brault M, Marty J C, Saliot A. 1984. Fatty acids from particulate matter and sediment in hydrothermal environments from the east Pacific rise, near 13°N. Org Geochem, 6: 217–222

Chernova T G, Rao P S, Pikovskii Y I, et al. 2001. The composition and source of hydrocarbons in sediments taken from the tectonically active Andaman Backarc Basin. Indian Ocean Mar Chem, 75(1–2): 1–15

DeMets C, Gordon R G, Argus D F, et al. 1994. Effect of recent revisions to the geomagnetic reversal time scale on estimate of current plate motions. Geophys Res Lett, 21(20): 2191–2194

Elias V O, Simoneit B R T, Cardoso J N. 1997. Even N-alkane predominances on the Amazon shelf and a Northeast Pacific hydrothermal system. Naturwissenschaften, 84(9): 415–420

Huang Xin, Chen Shuai, Zeng Zhigang, et al. 2017. Characteristics of hydrocarbons in sediment core samples from the northern Okinawa Trough. Mar Pollut Bull, 115(1–2): 507–514

Kates M. 1997. Diether and tetraether phospholipids and glycolipids as molecular markers for Archaebacteria (Archaea). In: Eganhouse R P, ed. Molecular Markers in Environmental Geochemistry. Washington, DC: ACS Symposium, 35–48

Lein A Y, Peresypkin V I, Simoneit B R T. 2003. Origin of hydrocarbons in hydrothermal sulfide ores in the Mid-Atlantic Ridge. Lithol Miner Resour, 38(5): 383–393

Li Jiwei, Zhou Huaiyang, Peng Xiaotong, et al. 2011. Abundance and distribution of fatty acids within the walls of an active deep-sea sulfide chimney. J Sea Res, 65(3): 333–339

Morgunova I P, Ivanov V N, Litvinenko I V, et al. 2012. Geochemistry of organic matter in bottom sediments of the ashadze hydrothermal field. Oceanology, 52(3): 345–353

Morris R J, Culkin F. 1976. Marine lipids: analytical techniques and fatty acid ester analyses. Oceanogr Mar Biol Ann Rev, 14: 391–433

Peng Xiaotong T, Li Jiwei, Zhou Huaiyang, et al. 2011. Characteristics and source of inorganic and organic compounds in the sediments from two hydrothermal fields of the Central Indian and Mid-Atlantic Ridges. J Asian Earth Sci, 41(3): 355–368

Petrova V I, Batova G I, Kursheva A V, et al. 2010. Geochemistry of organic matter of bottom sediments in the rises of the central Arctic Ocean. Russ Geol Geophys, 51(1): 88–97

Simoneit B R T. 1977. Organic matter in eolian dusts over the Atlantic Ocean. Mar Chem, 5(4–6): 443–464

Simoneit B R T, Brault M, Saliot A. 1990. Hydrocarbons associated with hydrothermal minerals, vent waters and talus on the East Pacific Rise and Mid-Atlantic Ridge. Appl Geochem, 5(1–2): 115–124

Simoneit B R T, Lein A Y, Peresypkin V I, et al. 2004. Composition and origin of hydrothermal petroleum and associated lipids in the sulfide deposits of the Rainbow Field (Mid-Atlantic Ridge at 36°N). Geochim Cosmochim Acta, 68(10): 2275–2294

Simoneit B R T, Mazurek M A, Brenner S, et al. 1979. Organic geochemistry of recent sediments from Guaymas Basin, Gulf of California. Deep-Sea Res: A, 26(8): 879–891

Suzuki N, Sakata S, Kaneko N. 1987. Biomarker maturation levels and primary migration stage of neogene tertiary crude oils and condensates in the Niigata sedimentary basin, Japan. J Jpn Assoc Pet Technol (in Japanese), 52(6): 499–510

Tao Chunhui, Li Huaiming, Yang Yaomin, et al. 2011. Two hydrothermal fields found on the Southern Mid-Atlantic Ridge. Sci China: Earth Sci, 54(9): 1302–1303

Venkatesan M I, Ruth E, Rao P S, et al. 2003. Hydrothermal petroleum in the sediments of the Andaman Backarc Basin, Indian Ocean. Appl Geochem, 18(6): 845–861

Yamanaka T, Sakata S. 2004. Abundance and distribution of fatty acids in hydrothermal vent sediments of the western Pacific Ocean. Org Geochem, 35(5): 573–582

Zhang Qiling, Hou Zengqian, Tang Shaohua. 2001. Organic composition of sulphide ores in the Okinawa Trough and its implications. Acta Geol Sin, 75(2): 196–203